# Gamma-Ray Multiplicities and Fission Modes in $^{208}$Pb($^{18}$O,$f$)

G. G. Chubarian,[1,*] M. G. Itkis,[2] N. A. Kondratiev,[2] E. M. Kozulin,[2] V. V. Pashkevich,[3] I. V. Pokrovsky,[2]
A. Ya. Rusanov,[4] V. S. Salamatin,[2] and R. P. Schmitt[1]

[1]*Cyclotron Institute, Texas A & M University, College Station, Texas 77843*
[2]*Flerov Laboratory of Nuclear Reactions, Joint Institute for Nuclear Research, 141980 Dubna, Russia*
[3]*Bogoliubov Laboratory of Theoretical Physics, Joint Institute for Nuclear Research, 141980 Dubna, Russia*
[4]*Institute of Nuclear Physics of the National Nuclear Center of Kazakhstan, 480082 Alma-Ata, Kazakhstan*

(Received 6 February 2001; published 10 July 2001)

Two components in the $M_\gamma(M)$ distribution were established in detailed measurements of mean $\gamma$-ray multiplicities from fission fragments of $^{226}$Th. For the first time in the $M_\gamma(M)$ dependencies we were able to distinguish two components associated with primary and the final (after the neutron evaporation) fission fragments, and show that at the scission point $M_\gamma$ is extremely sensitive to symmetric and asymmetric modes of fission. Theoretical calculations of the pre-scission shapes of the fissioning nuclei confirm our conclusions.

DOI: 10.1103/PhysRevLett.87.052701 PACS numbers: 25.85.Ge, 25.70.Jj, 27.90.+b

A few years ago we started a series of experiments to investigate carefully the properties of low-energy fission of the neutron-deficient Th isotopes. These nuclei are transitional between well-known groups near the Pb isotopes [1] and the traditionally measured heavy compound systems with $A > 226$ [2]. The investigations of the fission cross sections and the fission fragment mass-energy distributions (MED) of $^{220,224,226}$Th and $^{220}$Ra were presented in [3]. The new, multicomponent decomposition method of mass distributions was introduced in [4]. Recently, based on this method a detailed analysis of the fission fragment mass distributions of $^{226}$Th isotopes was performed in [5]. A given compound system was formed in the $^{18}$O + $^{208}$Pb reaction at a beam energy $E_{\rm lab}(^{18}{\rm O}) = 78$ MeV. This corresponds to a CN excitation energy $E^* = 26$ MeV. It was shown experimentally that the mass distribution has a complex three-humped structure with a central symmetric part and asymmetric shoulders with approximately 25% input in overall yield. As a result of the multicomponent analysis of the MED's four distinct fission modes were found. According to terminology introduced by Brosa [6] these are symmetric mode ($S$) and three asymmetric modes, standard-1 ($S1$), standard-2 ($S2$), and standard-3 ($S3$). Earlier it was found that fission modality exhibits itself not only in properties of MED's, but also in the fission fragment angular distributions [7], postfission neutron multiplicities $\nu_{\rm post}$ and their distributions [8,9]. In this Letter we will show that the phenomenon of multimodal fission also manifests itself in the $\gamma$-ray multiplicities ($M_\gamma$) from fission fragments of the neutron-deficient $^{226}$Th isotope.

The complex structure of the $M_\gamma(M)$ distributions from fission fragments in spontaneous fission of $^{252}$Cf and the thermal neutron induced fission of $^{235}$U and $^{239}$Pu were observed a long time ago [2,10]. In the experiments [11,12] the total $M_\gamma$ from both fission fragments was measured in spontaneous fission of $^{252}$Cf, and in the $^{232}$Th$(\alpha, f)$ reaction correspondingly. These measured $M_\gamma(M)$ distributions were very different. In symmetric fission of $^{252}$Cf a minimum in $M_\gamma$ was observed at symmetry in contrast to that in fission of $^{236}$U, where $M_\gamma(A_{\rm CN}/2)$ reached its maximum. On the other hand, in a heavy ion induced reaction [13] the fissioning nuclei are heated so much that the shell structure properties can be neglected. The MED's of the fission fragments have only one $S$ mode. However, in the $M_\gamma(M)$ dependence minima are observed around the magic number of protons $Z \cong 50$ and 28 or neutrons $N \cong 82$ and 50.

Measurements of the $\gamma$-ray multiplicities in coincidence with the fission fragments in $^{18}$O + $^{208}$Pb reaction at $E_{\rm lab}(^{18}{\rm O}) = 78$, 90, 117, 144, and 198 MeV will be discussed in this Letter. Experiments were mainly conducted on the K500 superconducting cyclotron at Texas A&M University Cyclotron Institute with the exception of the reaction with a lowest beam energy of 78 MeV, which was carried out on the Tandem at LNS in Catania (Italy). The latter was earlier reported in [3]. In the experiments time-of-flight spectrometer DEMAS-3 [14] was used. A well-known method of kinematically correlated coincidences was utilized for the registration and the identification of the fission fragments [15]. The spectrometer consisted of four "stop" parallel plate position-sensitive avalanche counters (PSAC) with $30 \times 20$ cm$^2$ sensitive area and two small $3 \times 4$ cm$^2$ "start" parallel plate avalanche counters (PPAC). PPAC's and PSAC's were positioned 4 and 40 cm from the target correspondingly. The spectrometer had a typical 0.2° angular and 250 ps time resolution. The estimated mass resolution was about 3–5 amu [3,14]. The $\gamma$-ray multiplicities were measured with an array of six $3 \times 3$ in NaI detectors arranged symmetrically around the target at the distance of 14 cm and at an angle of 55° out of the reaction plane.

The typical fission fragments MED's are shown in Figs. 1a–1f. At $E_{\rm lab} = 78$ MeV in the mass distributions (MD) the asymmetric component in fission is clearly visible (Fig. 1a). It tends to have a higher total kinetic energy $E_k$ for the mass range $M_H > 125$ (Fig. 1c). In

  

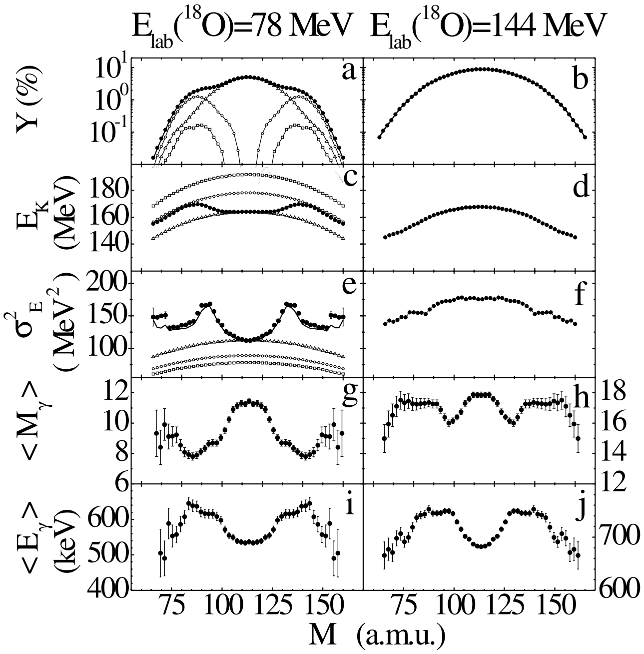


FIG. 1. From top to bottom: Experimental yields $Y$ of fission fragment masses (solid symbols) obtained at beam energies $E_{lab} = 78$ and 144 MeV and results of the decomposition (open symbols). The triangles correspond to the symmetric mode $S$, the circles—to mode $S2$, squares—to modes $S1 + S3$ (see text). Distributions of the total kinetic energy $E_K(M)$ as a function of the fission fragment mass and its decomposition (the same designations). Dependence of the variance $\sigma_E^2(M)$ of the fission fragment total kinetic energy on the mass, its decomposition, and its description (the solid curve). Smooth lines through the data points are for guidance only. For $E_{lab} = 144$ MeV only $S$ mode is realized. Gamma-ray multiplicities $M_\gamma(M)$ and their relative energies $E\gamma(M)$ as a function of the fission fragment masses.

the mass range $M_H = 130-134$ a well defined peak can be observed in the most sensitive characteristic of the fission modes: the dispersion of total kinetic energy as a function of mass $\sigma_E^2(M)$ (Fig. 1e). In the same figure, for the energy $E_{lab} = 78$ MeV the decomposition of MED on $S$, $S2$, and $S1 + S3$ modes done within method [4] is shown. For the energy $E_{lab} = 144$ MeV the MED's are completely different. Single Gaussian shape of the MD, and parabolic shapes of $E_K(M)$ and $\sigma_E^2(M)$ testify to the disappearance of shell effects. Such behavior of heated nuclei is predicted by the liquid drop model (LDM) [16] or the diffusion model [17]. In other words, only $S$ mode is realized in the fission of the heated nuclei.

At this point it is important to note that from the preliminary results [18] in the investigated reaction at $E_{lab} =$ 78 MeV the compound system is emitting approximately 1.5 prefission neutron $\langle \nu_{pre} \rangle$. This means that at the scission point we will have compound nuclei close to $^{224}$Th with approximately 13 MeV less excitation energy. There are no direct experimental results on $\langle \nu_{pre} \rangle$ for the same reaction at $E_{lab} = 144$ MeV, but for a close reaction $^{16}O$ + $^{208}$Pb at $E^* = 87$ MeV the number of pre-scission neutrons $\langle \nu_{pre} \rangle \cong 4$ [19]. Then at the scission point we will have $^{222}$Th. Below it will be shown that these circumstances do not affect the analysis and the interpretation of the experimental results. Finally, the time-of-flight method of measurements does not require any corrections of $Y(M)$ and $M_\gamma(M)$ on $\langle \nu_{post} \rangle$. This is important because the $\gamma$ rays are emitted from completely separated fission fragments at the very final stage of their deexcitation.

In Figs. 1g–1j the $\gamma$-ray multiplicities $M_\gamma(M)$ and their relative energies $E_\gamma(M)$ as a function of the fission fragment masses are shown. In the presented distributions significant differences may be noticed not only on the absolute values of $M_\gamma$ as a result of different temperatures $T$ and angular momenta $l$ of fissioning nuclei [13,16,20,21], but most important, in the structures of $M_\gamma(M)$ distributions at different beam energies. For the lowest beam energy $E_{lab} = 78$ MeV, where in the MD the asymmetric fission is observed, in the $M_\gamma(M)$ distributions (Fig. 1g) three groups of masses can be clearly noticed: first, around the symmetric fission $M = (A/2) \pm 8$ with high $\langle M_\gamma \rangle \cong \text{const} \cong 11.4$; second, with the local minimum at $M_H = 128-130$; and third, with the lowest $\langle M_\gamma \rangle \cong 8$ for the masses around $M_H = 140$. As was mentioned above, at the beam energy $E_{lab} = 144$ MeV the properties of the MED's correspond to the LDM approximation and are not sensitive to the shell effects. Nevertheless, the $M_\gamma(M)$ distributions (Fig. 1h) still have a structure. There still is a valley with a minimum at $M_H \cong 128-130$, but the second minimum around $M_H \cong 140$ is transformed into a wide plateau with almost the same $\langle M_\gamma \rangle$ value as for the symmetric part. In the $E_\gamma(M)$ distributions (Figs. 1i–1j) the situation is reversed. For mass ranges where the $\gamma$-ray multiplicities are low, their relative energies reach the highest values. For intermediate beam energies $E_{lab} = 90$, 117 MeV a smooth transition of structural peculiarities for lowest $E_{lab} = 78$ MeV to higher $E_{lab} = 144$ MeV beam energies is observed. At $E_{lab} = 144$ MeV and $E_{lab} = 198.5$ MeV the structures in $M_\gamma(M)$ are very similar. Thus, the gradual disappearance of asymmetric modes in MED corresponds to simultaneous disappearance of minimum around $M_H \cong 140$ in $M_\gamma(M)$ distributions.

It is well known that the $\gamma$ rays are emitted from the fission fragments after evaporation of postscission neutrons $\nu_{post}$ at the very last stage of their deexcitation. At this point the internal structure of fission fragments is very important. If the number of nucleons in the final fragment is close to the magic numbers, for example, $Z_H \sim 50$, $N_H \sim 82$, or $N_L \sim 50$, then the $\gamma$-ray cascade will reflect the structure of the nuclear states peculiar to near magic, almost spherical nuclei. These nuclei have minimal densities of quasiparticle and rotational excited states [22] and as a result the minimal value of $\langle M_\gamma \rangle$ will be observed relative to the nonmagic neighboring nuclei. This will take place even if the initial fragment is heated and strongly deformed [13].

On the other hand, during the spontaneous or low-energy fission at the scission point fragments can already be spherical, especially for the asymmetric modes $S1$ and $S2$ [5,23]. In this case the densities of quasiparticle and rotational excited states are already minimal; therefore for these fragments (modes) $\langle M_\gamma \rangle$ will be minimal in comparison to the other modes.

The set of calculated pre-scission deformations for cold and heated (up to $E^* = 75$ MeV) $^{224,222}$Th nuclei is shown in Fig. 2. Nuclear shapes are shown for the symmetric fission and ratios of masses 140/84 or 140/82, which correspond to the minimum of the fission valley on the potential energy surface for $S2$ mode, dominating the asymmetric mode at $E_{\mathrm{lab}} = 78$ MeV (Fig. 1). The details of pre-scission deformation calculations are given in [5,23].

In the present experiment $\langle M_\gamma \rangle$ from both fission fragments was measured, so only the summarized deformation at scission point may be discussed. As is shown in Fig. 2 in the case of low-energy fission the summarized deformation of both fragments for $S2$ mode ($\langle M_H \rangle = 140$) is significantly less than for both heated nucleus or symmetric $S$ mode of cold nucleus. On the other hand, according to the modern ideas about fission modes, fission fragments with the same mass can be formed in symmetric, as well as in asymmetric, valleys which is essential to those mode summarized deformations [1,3–6].

Generalizing all of the above, we can conclude that experimentally measured $M_\gamma$ may have two sources: primary fission fragments, if their structure of excited states is close to the final ones (asymmetric modes), and deexcited final fission fragments with their internal quasiparticle and rotational degrees of freedom, even if these fragments have the same nucleonic composition.

Now let as return to Fig. 1. At the beam energy $E_{\mathrm{lab}} = 144$ MeV at the scission point all fission fragments are strongly heated and deformed, and their internal structure is insignificant. That is why the minima in $M_\gamma(M)$ at $M_H = 128-130$ (and complementary to them) might be associated with the structure of fragments around the magic numbers $Z_H \sim 50$, $N_H \sim 80$, and $N_L \sim 50$. For all other masses there is no structure because they are far from the double-magic numbers. The minimum in $M_\gamma(M)$ around masses $M_H = 128-130$ appears for all measured energies and is connected with the properties of the fission fragments in their final stage. Another minimum around $M_H = 138-140$ at lower beam energies reflects the existence of close to spherical shapes in the heavy primary fragments near the scission point ($S2$ mode, Fig. 2). In this case the light fragment is deformed. Nevertheless, the total deformation of both fragments is significantly less than for the same mass range with higher excitation energies. In favor of this assumption is the fact that $S2$ mode is dominating during the fission of $^{226}$Th and has a yield almost 1 order of magnitude greater than the sum of $S1 + S3$ (Fig. 1). If we compare the structural peculiarities of the $M_\gamma(M)$ dependencies for both energies and also take into account the overall increase of $M_\gamma$ with excitation energy,

$$\Delta M_\gamma(M) = M_\gamma(M)|_{78} - [M_\gamma(M)|_{144} - 6.4], \qquad (1)$$

we will get the "pure" input of the fission modes in the structure of the $M_\gamma(M)$ distributions and will exclude events associated with the final properties of the fission fragments. In Eq. (1) 6.4 is the difference of the $\gamma$-ray multiplicities for the symmetric $S$ mode at the two beam energies. The difference of the $\gamma$-ray multiplicities $\Delta M_\gamma(M)$ is presented in Fig. 3. Since $S$ and $S2$ modes are dominating and the input of $S1 + S3$ modes is negligible, the $\Delta M_\gamma(M)$ distribution was approximated according to

$$\Delta M_\gamma(M) = \Delta M_\gamma^S(M) P^S + \Delta M_\gamma^{S1+S2+S3}(M) P^{S1+S2+S3}, \qquad (2)$$

where $M_\gamma^i$ ($i = S, S1 + S2 + S3$) is a $\gamma$ multiplicity for the mode $i$, and $P^i$ is the relative probability of the given mode yield obtained from decomposition of MED in Fig. 1. For $S$ mode we assumed that $M_\gamma^S$ does not depend on $M$ and equals 11.4. From Fig. 3 it is clear that $M_\gamma^S(M)$ is significantly higher than $M_\gamma^{S1+S2+S3}(M)$. Now if we assume that the fission fragments are deexciting through $E2$ transitions, then the mean $\gamma$-ray multiplicities

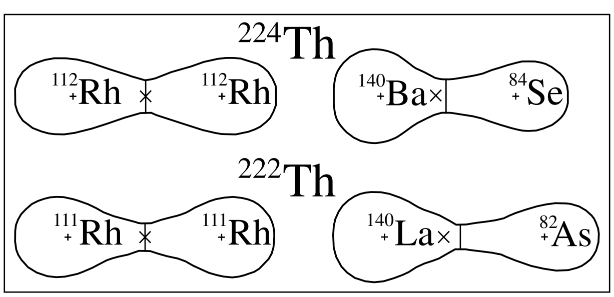


FIG. 2. Theoretical calculations of pre-scission shapes for the "cold" fission of $^{224}$Th (upper part), and for the "hot" fission of $^{222}$Th (lower part).

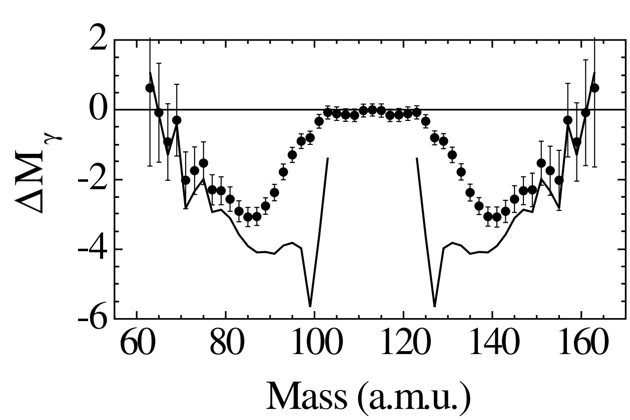


FIG. 3. The difference of the gamma-ray multiplicities (dots) $\Delta M_\gamma(M)$ and its decomposition on $S$, $S1 + S2 + S3$ components in accordance with Eq. (2) (solid line), as a function of fission fragment mass.

characterize their spin [10,13,16,20,21]. The spin value according to [22,24] depends directly on the deformation of fragments. From the data in Fig. 3 we can conclude that the mean value of the fragment spin at the scission point for $S2$ mode is substantially smaller than for $S$ mode. This may be evidence that the concept of the valley structure of the potential energy surface is a universal tool for an explanation of properties of a fissioning nucleus and fission fragments at the same time.

Thus, for the first time in the $M_\gamma(M)$ dependencies, for neutron-deficient thorium isotopes, we were able to distinguish two components associated with primary and the final (after the neutron evaporation) fission fragments, and show that at the scission point $M_\gamma$ is extremely sensitive to symmetric and asymmetric modes of fission.

The work has been supported by the U.S. Department of Energy under Grant No. DE-FG03-93ER40773, by the National Science Foundation under Grant No. PHY-9603143, by the Russian Foundation for Basic Research under Grant No. 99-02-17891, and by INTAS under Grant No. 97-11929.

*On leave from FLNR, JINR, Dubna, Russia.

[1] M. G. Itkis *et al.,* Z. Phys. A **320**, 433 (1985); , Sov. J. Part. Nucl. **19**, 301 (1988); Nucl. Phys. **A502**, 243c (1989).
[2] R. Vandenbosch and J. Huizenga, *Nuclear Fission* (Academic Press, New York, 1973); F. Gönnenwein, in *The Nuclear Fission Process,* edited by C. Wagemans (CRC Press, Boca Raton, FL, 1991), p. 287.
[3] G. G. Chubarian *et al.,* in *Proceedings of the Fourth International Conference on Dynamical Aspects of Nuclear Fission, (DANF'98), Časta-Papiernička, Slovak Republic, 1998,* edited by Yu. Ts. Oganessian *et al.* (World Scientific, Singapore, 2000), p. 293; I. V. Pokrovsky *et al.,* Phys. Rev. C **60**, 041304 (1999).
[4] S. I. Mulgin *et al.,* Phys. Lett. B **462**, 29 (1999).
[5] I. V. Pokrovsky *et al.,* Phys. Rev. C **62**, 014615 (2000).
[6] U. Brosa *et al.,* Phys. Rep. **197**, 167 (1990); P. Siegler *et al.*, Nucl. Phys. **A594**, 45 (1995).
[7] F. Steiper *et al.,* Nucl. Phys. **A563**, 282 (1993); A. A. Goverdovski *et al.,* Phys. At. Nucl. **58**, 188 (1995).
[8] J. van Aarle, *et al.,* Nucl. Phys. **A578**, 77 (1994); in *Second International Workshop Nuclear Fission and Fission Product Spectroscopy, Seyssins, France, 1998,* edited by G. Fioni *et al.,* AIP Conf. Proc. No. 447 (AIP, Woodbury, New York, 1998), p. 283.
[9] J. F. Wild *et al.,* Phys. Rev. C **41**, 640 (1990); T. Ohsawa *et al.,* Nucl. Phys. **A653**, 17 (1999); **A665**, 3 (2000).
[10] D. C. Hoffman and M. M. Hoffman, Annu. Rev. Nucl. Sci. **24**, 151 (1974); H.-H. Knitter *et al.,* in *The Nuclear Fission Process* (Ref. [2]), p 497; I. Ahmad and W. R. Phillips, Rep. Prog. Phys. **58**, 1415 (1995).
[11] P. Glassel *et al.,* Nucl. Phys. **A502**, 315c (1989).
[12] H. Hamagaki *et al.,* J. Phys. Soc. Jpn. **54**, 2453 (1985).
[13] R. P. Schmitt *et al.,* Z. Phys. A **321**, 411 (1985); J. R. Leigh *et al.,* Phys. Lett. B **159**, 9 (1985).
[14] M. G. Itkis *et al.,* in *Heavy Ion Physics Scientific Report 1993–1994* (JINR, FLNR, Dubna, 1995) p. 179; in *Tours Symposium on Nuclear Physics III, Tour, France, 1997*, edited by M. Arnould *et al.,* AIP Conf. Proc. No. 425 (AIP, Woodbury, New York, 1998), p. 189.
[15] J. Töke *et al.,* Nucl. Phys. **A440**, 327 (1985); G. G. Chubarian *et al.,* Phys. At. Nucl. **56**, 286 (1993).
[16] J. R. Nix and W. J. Swiatecki, Nucl. Phys. **71**, 1 (1965).
[17] G. D. Adeev *et al.,* Sov. J. Part. Nucl. **19**, 529 (1988); Nucl. Phys. **A502**, 405c 1989).
[18] M. G. Itkis *et al.* Nucl. Phys. **A654**, 870c (1999); A. Kelic *et al.,* Europhys. Lett. **47**, 552 (1999).
[19] H. Rossner *et al.,* Phys. Rev. C **45**, 719 (1992); D. Hilscher and H. Rossner, Ann. Phys. (Paris) **17**, 471 (1992).
[20] R. P. Schmitt *et al.,* Nucl. Phys. **A427**, 614 (1984); B. B. Back *et al.,* Phys. Rev. C **41**, 1495 (1990); R. K. Choudhury *et al.,* Phys. Rev. C **60**, 054609 (1999).
[21] L. G. Moretto and R. P. Schmitt, Phys. Rev. C **21**, 204 (1980); R. P. Schmitt and A. J. Pacheco, Nucl. Phys. **A379**, 313 (1982).
[22] A. V. Ignatyuk, *Statistical Properties of Excited Atomic Nuclei* (Energoatomizdat, Moscow, 1983), p. 71 [translated as IAEA report, INDC(CCP)-233/L, Vienna, 1985].
[23] Yu. V. Pyatkov *et al.,* Nucl. Phys. **A624**, 140 (1997).
[24] J. O. Rasmussen *et al.,* Nucl. Phys. **A316**, 465 (1969); M. Zielinska-Pfabe and K. Dietrich, Phys. Lett. **49B**, 123 (1974); I. N. Mikhailov and P. Quentin, Phys. Lett. B **462**, 7 (1999).